

Enhancing Effect of Glucose Microspheres in the Viability of Human Mesenchymal Stem Cell Suspensions for Clinical Administration

Patricia Gálvez · Maria J. Martín · Ana C. Calpena · Juan A. Tamayo · Maria A. Ruiz · Beatriz Clares

Received: 4 March 2014 / Accepted: 10 June 2014 / Published online: 25 June 2014
© Springer Science+Business Media New York 2014

ABSTRACT

Purpose A critical limiting factor of cell therapy is the short life of the stem cells. In this study, glucose containing alginate microspheres were developed and characterized to provide a sustained release system prolonging the viability of human mesenchymal stem cells (hMSCs) in a suspension for clinical application.

Methods The glucose microspheres were satisfactorily elaborated with alginate by emulsification/internal gelation method. Particle size was evaluated by light diffraction and optical microscopy. Shape and surface texture by scanning electron microscopy (SEM). Zeta potential, infrared spectra and release studies were also conducted. Also, rheological properties and stability of hMSCs suspensions with microspheres were tested. The viability of hMSCs was determined by trypan blue dye exclusion staining.

Results Microspheres of 86.62 μm , spherical shaped and -32.54 mV zeta potential with excellent stability, good encapsulation efficiency and providing an exponential release of glucose were obtained. hMSCs had better survival rate when they were packed with glucose microspheres. Microspheres maintained the aseptic conditions of the cell suspension without rheological, morphological or immunophenotypic disturbances on hMSCs.

Conclusions Developed microspheres were able to enhance the functionality of hMSC suspension. This strategy could be broadly applied to various therapeutic approaches in which prolonged viability of cells is necessary.

KEY WORDS alginate · cell viability · internal gelation · mesenchymal stem cells · microspheres

ABBREVIATIONS

AIC:	Akaike's Information Criterion
EE:	Encapsulation Efficiency
FITC:	Fluorescein Isothiocyanate
FTIR:	Fourier Transforms Infrared Spectroscopy
hMSCs:	Human Mesenchymal Stem Cells
LC:	Loading Capacity
PBS:	Phosphate Buffered Saline
PE:	Phycoerythrin
PY:	Percentage Yield
SEM:	Scanning Electron Microscopy
TPB:	Thioglycollate Penase Broth
TSPB:	Tryptic Soy Penase Broth

P. Gálvez
Andalusian Centre for Molecular Biology and Regenerative Medicine (CABIMER), Seville, Spain

M. J. Martín · M. A. Ruiz · B. Clares (✉)
Department of Pharmacy and Pharmaceutical Technology, School of Pharmacy, University of Granada, Campus of Cartuja St., 18071 Granada, Spain
e-mail: beatrizclares@ugr.es

A. C. Calpena
Biopharmaceutical and Pharmacokinetics Unit, School of Pharmacy University of Barcelona, Barcelona, Spain

J. A. Tamayo
Department of Medicinal and Organic Chemistry, School of Pharmacy University of Granada, Granada, Spain

INTRODUCTION

Human mesenchymal stem cells (hMSCs) are a potential resource in various preclinical studies, screening and development of new drugs, and clinical applications in regenerative medicine (1, 2). Their anti-inflammatory, angiogenic, antithrombogenic and antiapoptotic properties make them valuable tools for potential application in cell therapy (3, 4). Current investigations focus on the search for effective treatments for a range of diseases such as diabetes (5), heart disease (6), neurodegenerative diseases (7), tissue regeneration and repair (8), *etc.* However, substantial barriers to clinical translation still exist and must be overcome to

realize full clinical potential. These barriers span processes including cell isolation, *ex vivo* expansion, differentiation, quality control, shelf-life of the stem cell in the final product for being marketed and therapeutic efficacy and safety (9, 10).

When hMSCs are used as drugs, the cells have to be viable at the time of administration (11), specifically viability should be greater than 80% (12), for this reason, in order to improve cell viability, and the study of optimal delivery systems is of great interest.

Notwithstanding the advent of current strategies to reach a better control of hMSCs viability, such as encapsulation of cells (13), cell injection therapy is still the most commonly used scaffold-free delivery method to treat a variety of diseases, including: immunodeficiencies, myocardial defects, cartilage damage, peripheral arterial disease, diabetes, and neurological disorders (14). Long term clinical success will in part be dependent on the cells that remain viable and that assume correct functionality post-administration. In this line, limited impact of cell therapy and failure to generate long term effects has been attributed largely to extensive cell death (15). Thus, cell delivery in injectable hydrogels (16), loaded into microcarriers (17), and cell sheets (18), or new packing media (19) have been developed with important influence on the cell viability rate (20). In spite of the interesting and significant advances in the field have already been achieved, some challenges still remain unsolved. Optimal shelf-life and thus prolong the cell-loaded system upon *in vivo* implantation seems to be a pending issue.

As a result of the short shelf-life of hMSCs, several clinical interventions to donors are needed to maintain the minimum number of units available for implantation at any given time. It also often impacts on the final sterility of the cellular product. This short shelf-life also causes organizational problems since it is necessary to coordinate a multidisciplinary professional team, including the patient in a few hours, because of decreasing cell viability over time.

The use of a scaffold material enables implementation of additional excipients to improve cell viability by secreting a specific molecule or protein. (21). This technology is based on the immobilization of ingredient within a polymeric matrix surrounded by a semipermeable membrane for the long-term release (22). Natural polymers such as alginates are the most studied and characterized for cell encapsulation technology (22). Alginate is a biomaterial that has been found to have numerous applications in biomedical science, particularly in the areas of wound healing, drug delivery, *in vitro* cell culture, and tissue engineering due to its favorable properties, including biocompatibility and ease of gelation. Alginate is intrinsically non-fouling, not cleavable by natural enzymatic digestion and does not support cell adhesion (23).

It has been shown that reduced levels of glucose and oxygen combined with other environmental conditions (*i.e.*,

decreased pH, cell aggregation) decreases the anabolic activity of cells (24). In contrary, high extracellular glucose or glycolytic intermediate concentrations can maintain cell viability to some extent whilst stimulating lactate production (25). However, a few studies have examined the influence of nutrient factors and excipients on the survival of stem cells, particularly in a cellular suspension.

Therefore, the present study aimed to develop biodegradable alginate microspheres secreting glucose to enhance and prolong the functionality of an hMSC suspension. Viability of cells was analyzed. Furthermore, a detailed evaluation of the elaboration and characterization processes has been performed to guarantee particle uniformity, reproducibility and optimum cell viability. To our knowledge, this is the first time that such strategy to enhance cellular shelf-life has been reported.

MATERIALS AND METHODS

Synthesis of Glucose Loaded Alginate Microspheres

Glucose loaded microspheres elaboration method was based on the well-known emulsification/internal gelation methodology with modification (26). The W/O emulsion was performed with a sodium alginate aqueous solution (Fagron Iberica, Terrassa, Spain) purified by filtration, extraction and precipitation (27). Calcium carbonate (Panreac Quimica, Barcelona, Spain) and glucose anhydrous (Guinama, Alboraya, Spain) were utilized as the internal phase, and vegetable oil (Guinama, Alboraya, Spain) as the external phase.

Briefly, 0.2 g of calcium carbonate was added to 40 mL solution of 50% (*w/w*) glucose and 5% (*w/v*) sodium alginate. After homogenization, the suspension was dispersed in 100 mL of vegetable oil (continuous phase) containing Span[®] 80, 2% (*w/v*), (Guinama, Alboraya, Spain). The mixture was stirred at 700 rpm for 10 min to form uniform water in oil (W/O) emulsion. Under stirring, 20 mL of vegetable oil containing 0.850 mL of glacial acetic acid (Panreac Quimica, Barcelona, Spain) was added to the W/O emulsion, to complete the calcium carbonate solubilization. After 10 min under stirring, pregelified microspheres were separated from the oil dispersion by mixing with calcium chloride solution 5% (*w/v*) (BDH Prolabo, Barcelona, Spain). The supernatant was discarded and the alginate microspheres were centrifuged and washed two times with double distilled water. After this, particles were collected and washed again in 100 mL double distilled water by vacuum filtration and stored at 4 ° C in Petri dishes. Glassware and reagents used in the experiments were sterilized before use.

Cell Isolation and Culture

Autologous hMSCs were isolated from abdominal adipose tissue biopsies. All donors provided informed consent that was formerly approved by local and regional medical research ethics committees (EudraCT 2010-019774-33). Each patient was appropriately screened and tested for human pathogens. In particular, the presence of Human Immunodeficiency Virus, hepatitis B and hepatitis C virus were analyzed.

Cells were isolated from human adipose tissue by enzymatic digestion with collagenase (2 mg collagenase/1 g adipose tissue) (Roche Pharma, Basel, Switzerland), centrifuged at 400 g for 10 min, filtered and washed with phosphate buffered saline (PBS) (Sigma-Aldrich, St. Louis, MO, USA) to obtain the stromal cells.

These cells were suspended and plated at medium density of $12\text{--}20 \times 10^4$ cells/cm² in culture flasks (Nunc A/S, Roskilde, Denmark) with expansion medium composed by Dulbecco's modified eagle's medium, supplemented with 10% fetal bovine serum, 1% of 10,000 IU/mL penicillin, 10 mg/mL streptomycin, 2% of 200 mM L-alanine solution and 1% of 200 mM L-glutamine, (all from Sigma-Aldrich, St. Louis, MO, USA). After 24 h, non-adherent cells were removed by replacing the expansion medium. The medium was replaced every 2 or 3 days a week. Cells were harvested upon reaching 80% confluence, and subcultured using 0.25% trypsin (Invitrogen, Grand Island, NY, USA) in expansion medium, and plated at medium density, 3,500–5,500 cells/cm². Cells were cultured under 95% relative humidity, at 37°C and 5% CO₂. Three different processes of *ex vivo* expansion hMSCs were carried out (named 1, 2 and 3) from passages 3–4 to analyze their microbiological quality.

Cells were finally packed at concentration of 1×10^6 cells/mL with 1 mL of packaging medium consisting of 50% glucose 5%, 45% lactated Ringer's solution and 55% albumin 20% (Grifols, Barcelona, Spain). hMSCs were packed in 10 mL Luer-lock syringes (Becton Dickinson & Co., Franklin Lakes, NJ, USA) at 4°C (19).

Physicochemical Characterization of Microspheres

Morphological and Particle Size Analysis

Morphology of hydrated microspheres was first monitored by optical microscopic observation using an optical microscope Olympus BX40 microscope equipped with a calibrated eyepiece micrometer and camera Olympus SC35 (Tokyo, Japan) under a magnification of 100×.

Particle size distribution was confirmed by light diffraction (LD) using a LS 13 320 analyzer (Beckman coulter Inc., Brea, CA, USA) with a size range from 0.04 to 2,000 μm yielding the volume distribution of the particles. Characterization parameters were the diameters LD_{0.1}, LD_{0.5} and LD_{0.9}, namely

the particle diameters determined at the 10th, 50th and 90th percentile of the undersized particle distribution curve. A diameter LD_{0.5} of 1 μm means that 50% of all particles possess a diameter of 1 μm or less. Equally, mean diameter over the volume distribution (LD_{4.5}) and polydispersity expressed as the Span factor were also calculated (28).

The shape, surface texture and internal structure of the microspheres were examined by scanning electron microscopy (SEM) using a Zeiss DSM 950 microscope (Carl Zeiss AG, Oberkochen, Germany).

Zeta Potential

The surface electrical properties of cell and microspheres suspension ~0.1% (*w/v*), were analyzed by electrophoresis measurements in double distilled water using a Zetasizer 2000 (Malvern Instruments Ltd., Malvern, UK) electrophoresis device. Final zeta potential (ζ) values calculated from the electrophoretic mobility by the Helmholtz–Smoluchowski equation were average values from nine measurements made on the same sample at 25.0 ± 0.5°C.

Fourier Transforms Infrared Spectroscopy Measurement (FTIR)

Studies of infrared spectra of glucose, raw polymer, and microspheres were conducted with a FTIR UATR Two N 92052 spectrometer (Perkin Elmer, Waltham, MA, USA). Each sample was scanned over a wave number region of 400 to 4,500 cm⁻¹. The characteristic peaks were recorded.

Determination of Percentage Yield, Loading Capacity and Encapsulation Efficiency

The percentage yield (PY), loading capacity (LC) and encapsulation efficiency (EE) was calculated based on the dry weight of glucose and the alginate. EE was determined for all samples after the manufacturing process. Total glucose utilized was considered as the sum of encapsulated and non-encapsulated. Determination of glucose level was performed as follows, 0.5 g of particles at 25°C was added to PBS (0.1 M, pH 7, Sigma-Aldrich, St. Louis, MO, USA); the mixture was liquefied by gently shaking for 30 min at room temperature. After that, all samples were filtered through a 0.22 μm filter (Teknokroma®, Barcelona, Spain) and analyzed with the kit for the detection of glucose (Spinreact, Girona, Spain), the colored reaction was measured in triplicate at 505 nm in a Lambda 40 spectrophotometer (Perkin Elmer, Waltham, MA, USA). Equally, for determination of the amount of glucose adsorbed in the microsphere surface, 0.5 g of each microcapsule was added to 50 mL double distilled water and maintained at 25.0 ± 0.5°C under mechanical stirring (50 rpm) for 48 h. Then solution was filtered through a 0.22 μm filter and analyzed in triplicate.

In vitro Glucose Release

In vitro release test was performed by suspending 1.25 g of glucose microspheres in 50 mL of the packaging medium in closed glass vials. Then vials were stored at 4°C for 72 h, sink conditions were maintained during the study. At each time point (24, 48 and 72 h), three vials were collected and vortexed, the content was filtered through a 0.22 µm filter (Teknokroma®, Barcelona, Spain) and the concentrations of the released glucose were determined in triplicate by using the kit as described above. In order to evaluate the *in vitro* release kinetics, first order polynomial and exponential growth mathematical models were used. The adequacy of the delivery profiles to the mathematical models was based on the highest correlation coefficient value (r^2) and the smallest Akaike's Information Criterion (AIC), $[AIC = n \times \ln SSQ + 2p]$, as indicator of the model's suitability for a given dataset (29). Where n is the number of pairs of experimental values, SSQ is the residuals sum of squares and p is the number of parameters in the fitting function. The study was conducted using the software Prism®, v. 3.00 (GraphPad Software Inc., San Diego, CA, USA).

Determination of the Effect of Glucose Microspheres on Cell Viability

MSCs from passage 3 were used. Cells were harvested using 0.25% trypsin (Invitrogen, Grand Island, NY, USA) and centrifuged at 400 g for 10 min with expansion medium. The cell pellet was resuspended at concentration of 1×10^6 cells/mL with 1 mL of packaging medium. Four packaging media were prepared, medium A, containing glucose microspheres; medium B, microspheres without glucose (unloaded); medium C, glucose microspheres with phosphate buffer solution (0.1 M, pH 7); and medium D, control medium without microspheres. The excipients (Grifols, Barcelona, Spain) for 50 mL of each such media are reported in Table 1.

MSCs were packed in 10 mL Luer-lock syringes (Becton Dickinson and Company, Franklin Lakes, NJ, USA) and

stored at 4°C in a normal atmosphere. The stability study was based on the hMSCs viability every 6 h for 60 h.

Cell viability was determined by trypan blue dye exclusion staining and posterior counting of cells in a Neubauer chamber (30). Each sample was counted three times and the average (%) was calculated $[\% = \text{Number of viable cells} / \text{number of cells} \times 100]$.

Kinetic Evaluation of Stability

A kinetic evaluation of the cell viability was performed on the base of the obtained results. Experimental data were fitted to five different kinetic models: zero order, first order polynomial, second order polynomial, dual with shoulder and plateau decay zero, to find out the mechanism that statistically best represented our findings.

A nonlinear least-squares regression was performed using the Prism®, v. 3.00 software (GraphPad Software Inc., San Diego, CA, USA). The best model to describe the stability profile was selected based on the r^2 and AIC.

Microbiological Studies

Microbiological analysis was based on the study of the sterility of the cells before being packaged and after stability study with microspheres (60 h). The test was carried out by direct inoculation in accordance with the European Pharmacopoeia (31). 1 mL of each medium (A, B, C and D) was inoculated in two microbiological media: Thioglycollate Penase Broth 9 mL (TPB) to detect anaerobic and aerobic bacteria, and Tryptic Soy Penase Broth 9 mL (TSPB) (VWR International, Radnor, PA, USA), a soybean casein digest medium to detect fungi and aerobic bacteria. For each media (TPB and TSPB), sterility test and growth promotion test of aerobes, anaerobes and fungi were previously verified. The inoculated media were incubated for 14 days at 35 and 22°C, respectively. After 14 days, if there had been microbial growth, the medium would have shown turbidity. Negative controls were established by inoculating 1 mL of 0.9% sterile NaCl (bioMérieux, Marcy l'Etoile, France) in duplicate for each medium. The inoculated media were incubated for 14 days at 35 and 22°C (TPB and TSPB respectively). After 14 days, if there had been microbial growth, the medium would have shown turbidity. This assay was performed in aseptic conditions with an isolator HPI-4PI-S (Esco Technologies, Inc., Hatboro, PA, USA).

hMSCs Immunophenotypic Analysis

At passage 4, after stability study of the MSCs with glucose microspheres (Medium A) and with control medium (Medium D), immunophenotyping study of hMSCs was performed in order to identify the presence of specific surface antigens.

Table 1 Composition (mL) of Different Packaging Media (50 mL Final Volume)

Ingredients	Medium A	Medium B	Medium C	Medium D
Lactated Ringer's solution (mL)	22.5	22.5	21.5	22.5
Glucose 5% (mL)	25	25	25	25
Albumin 20% (mL)	2.5	2.5	2.5	2.5
Glucose loaded microparticles (g)	1.25	—	1.25	—
Unloaded microparticles (g)	—	1.25	—	—
Phosphate buffer solution (mL)	—	—	1	—

Between 2.5 and 5×10^5 cells were separated in 1.3 mL of expansion medium. The following markers were analyzed: CD13-PE, CD29-PE, CD90-FITC, CD105-PE, CD31-FITC, CD34-PE, CD45-FITC and HLA II-FITC (Becton Dickinson and Co., Franklin Lakes, NJ, USA). Mouse antibodies served as control: Isotype-FITC IgG1-k, Isotype-FITC IgG2a-k, Isotype-PE IgG1-k (all from Becton Dickinson and Co., Franklin Lakes, NJ, USA). One hundred μL of cell suspension were prepared with $5 \mu\text{L}$ of each of the following reagents: fluorescein isothiocyanate (FITC), phycoerythrin (PE) antibody and control, and incubated at 4°C for 20 min in the dark. Then, 3 mL of PBS (Sigma-Aldrich, St. Louis, MO, USA) were added to each cell suspension and centrifuged at 400 g for 10 min. Finally each cell pellet was diluted in $300 \mu\text{L}$ of PBS and $5,000$ labeled cells were analyzed using a FACSCalibur analyzer flow cytometer system running CellQuest Pro software (Becton Dickinson and Co., Franklin Lakes, NJ, USA), and the percentage of viable cells positive for each marker were determined.

Physicochemical Characterization of the MSCs –Microsphere Suspension

Morphological Analysis

Morphological characteristics of hMSCs were observed in each medium for the stability study by optical microscopy equipped by camera (Olympus, Tokyo, Japan). Each suspension (A, B, C and D) was observed at 4°C , each 24 h for 48 h to analyze the morphology and the cell aggregation.

Rheological Studies

The rheological characterization was performed at 25°C using a rotational rheometer HAAKE Rheostress 1 (Thermo Fisher Scientific, Karlsruhe, Germany) equipped with a parallel plate geometry set-up with fixed lower and upper plate (Haake PP60 Ti, 6 cm diameter). Different gaps between plates were tested and a separation of 0.105 mm was selected. The rheometer was connected to a computer provided with the software HAAKE Rheowin[®] Job Manager V. 3.3 to carry out the test and Rheowin[®] Data Manager v. 3.3 (Thermo Electron Corporation, Karlsruhe, Germany) to carry out the analysis of the obtained data. Viscosity curves and flow curves were recorded for 1 min during the ramp-up period from 0 to 100 s^{-1} , 1 min at 100 s^{-1} (constant share rate period) and finally 3 min during the ramp-down period from 100 to 0 s^{-1} . All determinations were performed in triplicate.

Data from the flow curves (when resulted to be non-Newtonian) were fitted to different mathematical models, Bingham, Ostwald-De-Waele, Herschel-Bulkley, Casson and Cross, using the Prism[®], v. 3.00 software (GraphPad Software Inc., San Diego, CA, USA).

Optical Characterization of the Stability

Light scattering methods are often used to study the stability of suspensions; an analysis of multiple dispersion of light was used to predict and confirm the physical stability of the cell suspensions using the TurbiScanLab[®] (Formulation, L'Union, France). The light source is a pulsed near infrared light source ($\lambda=880$ nm). Two synchronous optical sensors receive respectively light transmitted through the sample (0° from the incident radiation, transmission sensor), and light back-scattered by the sample (135° from the incident radiation, backscattering detector). Each undiluted formulation (20 mL) was placed and kept on a cylindrical glass measuring cell which was completely scanned by a reading head.

Statistical Analysis

Tests for significant differences between means were performed by Student's *t*-test or one-way ANOVA using the Prism[®], v. 3.00 software (GraphPad Software Inc., San Diego, CA, USA) followed by a Tukey's multiple comparison test. Differences where $P < 0.05$ were considered statistically significant. Experiments were repeated at least three times and results expressed as the mean \pm standard deviation (SD).

RESULTS

Microspheres Elaboration

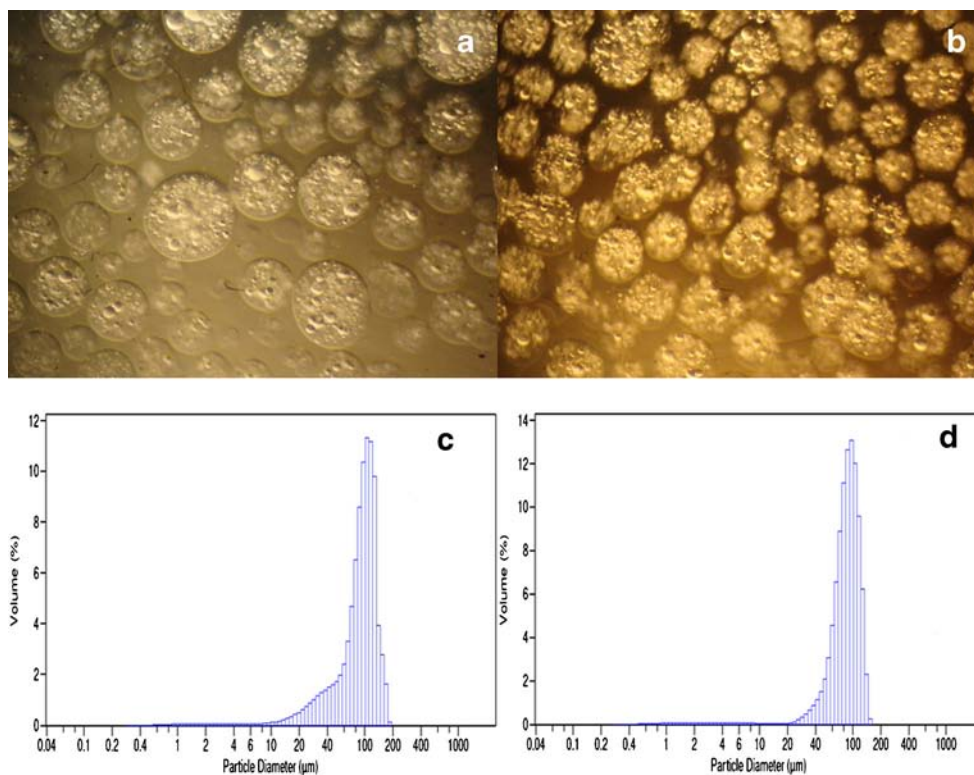
Gelation was achieved by gentle acidification of the alginate solution containing an insoluble calcium salt with an oil-soluble acid that causes calcium ion release, resulting spherical shaped and small sized alginate microspheres. Thus, it was a suitable procedure to encapsulate materials such as glucose which was first confirmed by optical microscopy (Fig. 1a and b).

Physicochemical Characterization of Microspheres

Size distribution values of microspheres are presented in Table 2, as well as the span factor. Both types of microspheres, unloaded and glucose loaded presented unimodal distribution with no secondary peaks (Fig. 1c and d). The mean particle sizes ($LD_{4.5}$) were 94.03 and $86.62 \mu\text{m}$ with Span factors of 1.06 and 0.77 for unloaded and glucose loaded microspheres, respectively. The SEM morphological evaluation (Fig. 2) showed homogeneous characteristics with sphericity without particle aggregation.

Measurements of ζ derived from photon correlation spectroscopy are shown in Table 2. Both types of microspheres exhibited negatives ζ values, -31.29 and -32.54 mV (plain

Fig. 1 Optical micrographs and volume distribution of alginate microspheres. Optical micrograph of unloaded microspheres (**a**), optical micrograph of glucose loaded microspheres (**b**), particle size distribution of unloaded microspheres (**c**) and particle size distribution of glucose loaded microspheres (**d**).



and glucose microspheres, respectively). The inclusion of the glucose did not significantly alter ζ .

Figure 3 shows the FTIR spectra graphs of glucose, unloaded microspheres and glucose loaded microspheres. Glucose displayed the following absorption bands: ν (O-H) between 3,570 and 3,120 cm^{-1} , ν (C-O) between 1,230 and 1,000 cm^{-1} , and ν (C-O-C) between 1,275 and 800 cm^{-1} . The two latter bands, the C-O region, are known to be the most specific of this molecule (32). Alginate showed different peaks: an antisymmetric stretch at 1,596 cm^{-1} and a symmetric

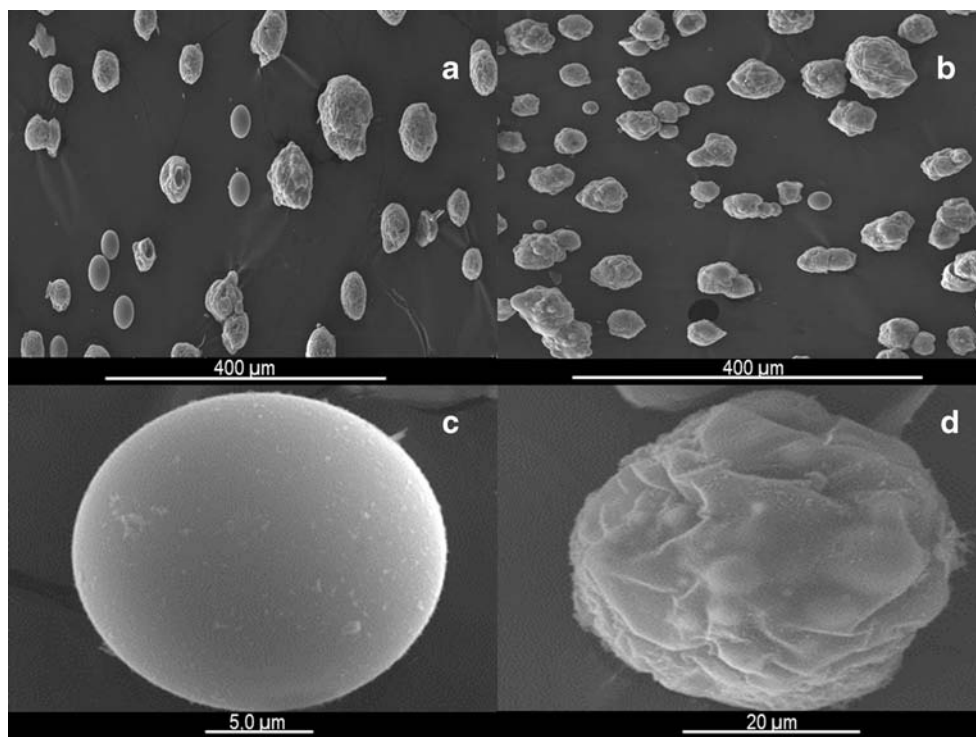
stretch at 1,412 cm^{-1} due to the carboxylate group (26). Cross-linking of alginate by Ca^{+2} was shown by a decrease in the wave number of the carbonyl peak from 1,650 to 1,465 cm^{-1} .

The values of PY, LC and EE of several batches of glucose loaded microspheres are listed in Table 2. Concretely, the main factors of the vehiculization of the glucose were 70.29, 20.45 and 30.54%, respectively. Compared to surface adsorption onto the preformed microspheres, the glucose entrapment into the polymeric shell resulted in a much better loading.

Table 2 Particle Size Distribution, Span and Zeta Potential of Microspheres. K is the Release Rate Constant, γ_0 is the Initial Percentage Drug Released at the Beginning of the Experiment and Doubling Timing is the Time it Takes to Double the % of Glucose Released

Parameter		Glucose microspheres	Unloaded microspheres
Volume distribution	LD _{4.3} ($\mu\text{m} \pm \text{SD}$)	86.62 \pm 27.19	94.03 \pm 37.49
	LD _{0.1} (μm)	53.19	37.19
	LD _{0.5} (μm)	87.89	97.90
	LD _{0.9} (μm)	120.50	140.70
Span factor		0.77	1.06
Zeta potential (mV \pm SD)		-32.54 \pm 1.91	-31.29 \pm 1.74
Encapsulation efficiency (%)	Surface	5.43 \pm 0.32	—
	Inside	25.11 \pm 5.51	—
Loading capacity (%)		20.45 \pm 3.74	—
Percentage yield (%)		70.29 \pm 2.61	—
Release parameters	γ_0 (%)	4.056	—
	K (h^{-1})	0.044	—
	Doubling timing (h)	15.57	—

Fig. 2 Scanning electron microscope micrographs of unloaded alginate microspheres (a and c) and glucose loaded alginate microspheres (b and d).



In vitro Release of Glucose from Microspheres

Glucose loaded microspheres were subjected to *in vitro* release studies in the presence of packaging media. Figure 4 shows the release pattern, within 24 h, 13.81 ± 4.61% of glucose was released from the microspheres. This release rate increased after 24 h and 48 h from 31.63 ± 11.22 to 100.45 ± 25.34%. It is expected that glucose release from cross-linked alginate microspheres occurred as a result of swelling and erosion of the polymer (33). Based on the above described experimental findings, various mathematical approaches were used to describe the observed *in vitro* release rates, exhibiting an increase

in growing velocity as time increases. The exponential growth model, defined as the mathematical equation $[y=y_0 \times e^{K \cdot x}]$ was the most appropriate to describe the kinetics of glucose release from elaborated microspheres with a r^2 of 0.9991 and AIC 14.17, where K is the release rate constant (h^{-1}) and y_0 is the initial percentage glucose released at the beginning of the experiment (%).

Kinetics parameters are reported in Table 2, in this context, doubling time is the period required to double the percentage of glucose released (h). The mathematical model shows an initial percentage of glucose released of 4.056 ± 1.022, which can be attributed to the

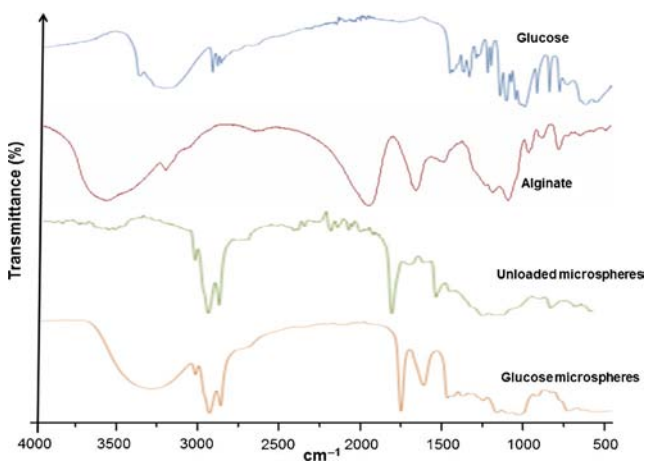


Fig. 3 FTIR spectra of glucose, alginate, unloaded alginate microspheres and glucose loaded alginate microspheres.

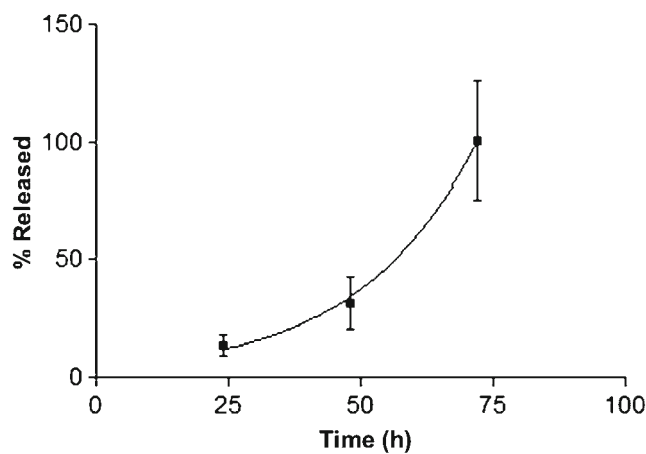


Fig. 4 Percentage glucose cumulative release from alginate microspheres (error bars ±SD, n = 3).

surface associated glucose (5.43 ± 0.32), followed by an exponential release.

Effect of Glucose Loaded Microspheres on Cell Viability

On passage 3, the average viability of the hMSCs cultured before packing was $95.1 \pm 1.2\%$. The same cells were packed in four different media (A, B, C, D) and the average viability decreased throughout the assay. Viability measurements are represented in Fig. 5a. Medium A showed that viability was greater than 90% for 30 h after packaging ($91.5 \pm 3.5\%$), however after 48 h viability declined below 80% (77.2 ± 2.7) as medium B ($76.3 \pm 3.5\%$). Medium C maintained the viability above 80% for less time, up to 36 h ($82.9 \pm 2.1\%$). Medium D showed that viability was greater than 80% for 48 h after packaging ($80.2 \pm 2.85\%$), however decreased more rapidly from 12 h.

According to the smallest AIC and r^2 value closest to 1, it was observed that second order polynomial model was the best to describe statistically the kinetic viability of medium A, B and C. On the other hand, first order polynomial was the most suitable for medium D.

Microbiological Studies

Sterility testing was performed on the hMSCs during culture (passage 3) and after stability study to ensure no contamination. When the incubation period had finished all samples were observed and no turbidity was exhibited, confirming the absence of contaminating microorganisms.

hMSCs Immunophenotypic Analysis

Analysis revealed that all populations (before and after packing with glucose microspheres) were positive ($>95\%$) for mesenchymal markers (CD13, CD29, CD90 and CD105) and negative ($<10\%$) for endothelial and hematopoietic lineage markers (CD34, CD45, CD31 and HLA-II) as is shown in Fig. 6. Fluorescence cytometry of MSCs, with or without microspheres showed no differences when the MSCs were stored at 4°C for 48 h.

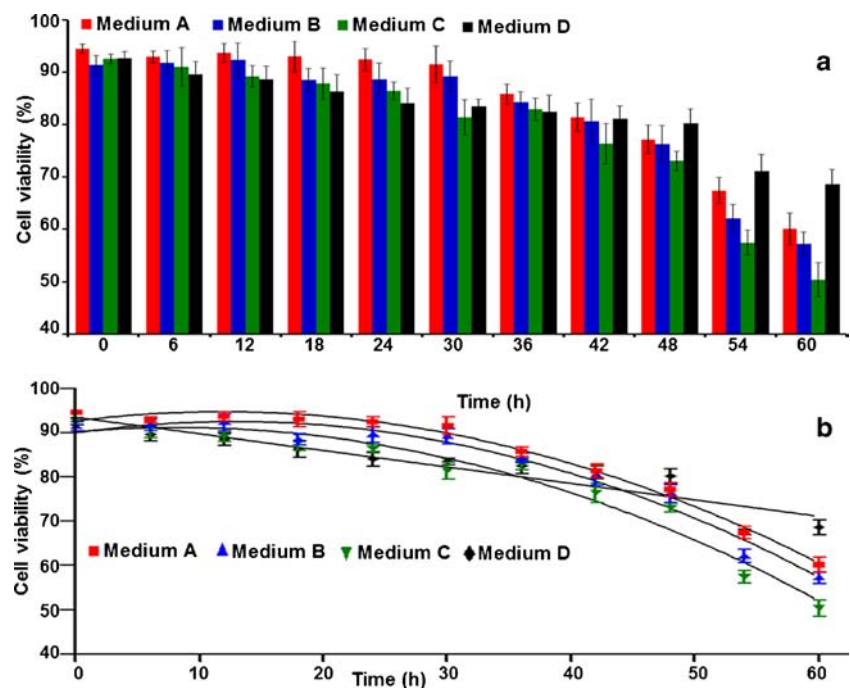
Physicochemical Characterization of the Final MSCs –Based Medicine

Rheological Studies

The flow and viscosity curves of the suspensions (shear stress *versus* shear rate, and viscosity *versus* shear rate) are shown in Fig. 7. The unstirred sample (Fig. 7a) exhibited Newtonian behavior and had lower viscosity value (1.011 ± 0.05 mPas), which indicated that there was migration of aggregates/flocculates.

Sample analyzed after shaking (Fig. 7b) exhibited a pseudoplastic behavior, where most aggregates were separated as a consequence of shear forces, which was sufficient to break-up the weak reversible flocculation. Viscosity value of the finished cell suspension in this case was 1.533 ± 0.044 mPas. Rheological data of this sample were fitted to mathematical models. Based on the lowest chi-square value and the r^2 closest to 1 (0.0021 and 0.9926, respectively), Cross model

Fig. 5 Cell viability in different media (a). Mathematical model graphs after fitting experimental data of cell viability over time (b).



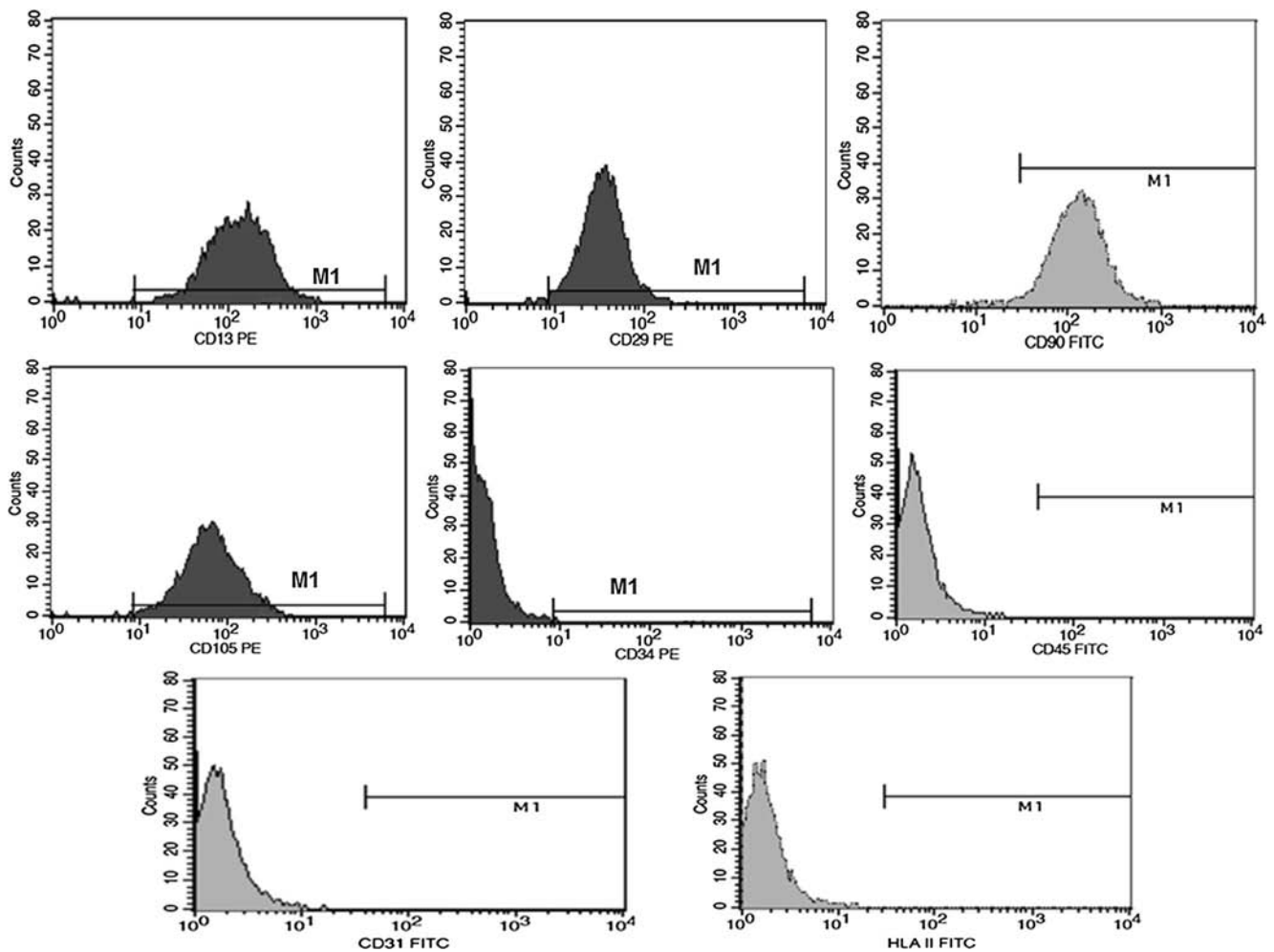


Fig. 6 Immunophenotypic characterization of the hMSCs suspension after incorporating glucose microspheres (Medium A) for 48 h at 4°C.

was statistically the best, showing that flow behavior was not influenced by time and/or temperature. However, Newton model provided the worst overall prediction of rheological behavior, 0.0088 (chi-square) and 0.9699 (r^2).

Morphological Analysis

To determine whether the hMSCs suspension with microspheres maintained their morphologic characteristics, they were tested after 48 h storage t in each medium at 4°C and before packing. The adherent cultured hMSCs exhibited a homogeneous population with a fibroblast-like morphology when observed under a light microscope before packing (Fig. 8). Interestingly, no morphological differences were found when the cells were packed with alginate.

Optical Characterization of the Stability

Fig. 9 shows backscattering profile of the final product containing hMSCs and glucose microspheres corresponding to measurements on different hours. The left side of the curves

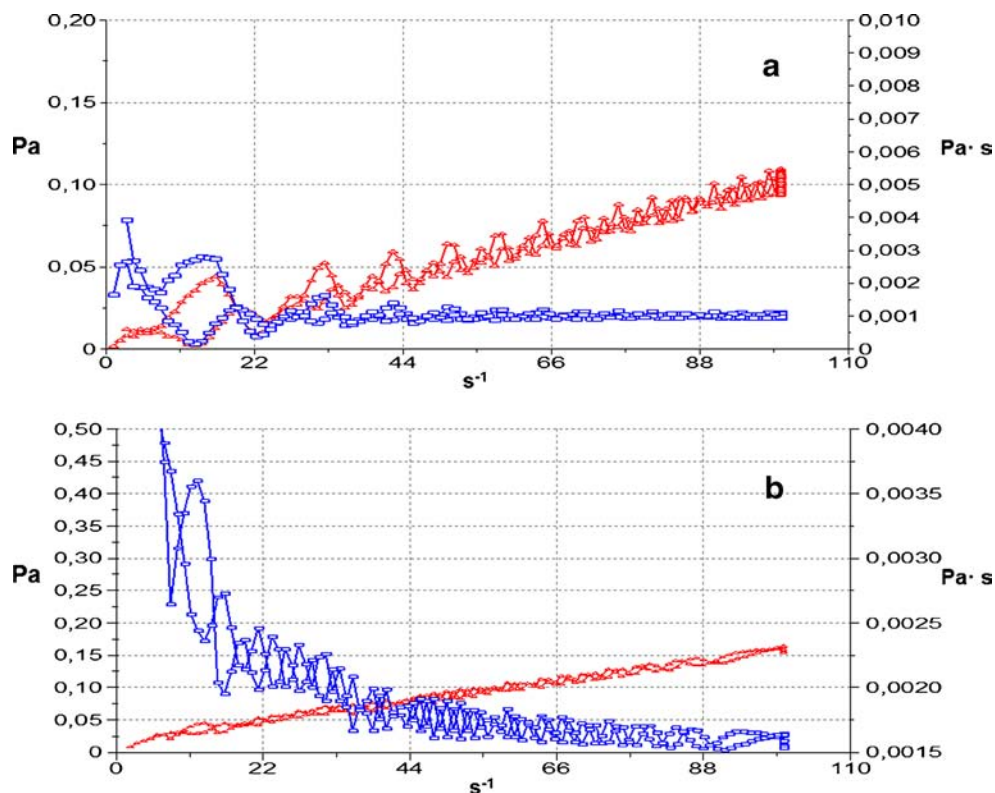
corresponds to the bottom of the vial, whereas the right side corresponds to the top. The region below 2 mm marks the metal base and the strong decay of backscattering above 48 mm the beginning of the free surface of the sample. Both creaming and flocculation mechanisms were involved. It can be observed that the initial dispersion presented a backscattering value about 5% and there were no changes in backscattering for the first 2 h. Between 2 and 24 h, a progressive backscattering was observed and suspension developed a “delayed” or “hindered” sedimentation.

DISCUSSION

An emulsification/internal gelation method is proposed for producing small diameter alginate microspheres. Importantly, alginate purified by a multi-step extraction procedure to a very high purity did not induce any significant foreign body reaction when implanted into animals (34).

The particle size analysis is an important factor in the characterization of the physical stability of colloidal dispersions.

Fig. 7 Cell suspension rheograms. It shows the shear stress (Pa) (in red) and the viscosity (Pa·s) (in blue). Unstirred sample (a), and stirred sample (b).



So, LD measurements were performed to investigate the influence of glucose incorporation on the microspheres dispersion. Increasing the internal phase with glucose led to a decrease on microspheres size, which agrees with other studies. In this line, it was verified that increasing internal phase ratio resulted in a slight decrease in mean size during hemoglobin encapsulation (35).

In this study, using the same methodology, these differences were further proven. During the elaboration method, an increase of viscosity is coupled with a reduction of microsphere size by the decreasing surface tension and emulsion stability enhancement (36). In concordance, the inclusion of the glucose in the alginate solution would result in such viscosity augmentation, and glucose loaded microspheres exhibited significantly smaller size. Moreover, the same effect was observed in the polydispersity with Span factor values for unloaded and loaded microspheres, indicating a slightly broader particle size distribution in unloaded microspheres.

The particle shape observed by SEM was more irregular than optical microscopy. This is due to the oil in the microspheres that leaked out from the shell which led to the shrinking and deformation of the microspheres (37). Unloaded microspheres showed slightly smoother surface (Fig. 2c) than glucose loaded (Fig. 2d). It could be justified by an increase in the frequency of collisions during emulsification process, resulting in a rough surface, due to a high viscosity of the internal phase, and thus a need of higher share force to

separate the oil phase into droplets. However, the agitation used to prepare the particles was the same in alginate and in glucose loaded microspheres.

The negative charge of microspheres could be attributed to the presence of polymeric terminal carboxylic groups provided by the acidic groups of alginate on the surface. A ζ less than -30 mV or higher than $+30$ mV can be an indicator to assure the stability of particulate systems. This ζ value could explain that aggregation phenomenon with cells was easily preventable, due to the electrostatic repulsion force between microsphere surface and cell (-12.07 mV).

Alginates present different proportions or alternating patterns of guluronic and mannuronic units. The presence of these acids can be identified from their characteristic bands: while the guluronic units originate a band at approximately $1,025$ cm⁻¹, the mannuronic units originate a band at approximately $1,100$ cm⁻¹. Thus, the guluronic/mannuronic concentration ratio can be inferred from the relative intensity ratio of the $1,025$ and $1,100$ cm⁻¹ bands. As it can be seen in Fig. 3 the alginate used in this study has higher proportion of guluronic. High mannuronic content alginates are immunogenic and approximately 10 times more potent in inducing cytokine production compared with high guluronic alginates (38). The spectra showed that the characteristic bands of unloaded microspheres are maintained in the loaded microspheres indicating that glucose did not induce subsequent modifications in the structure of alginate.

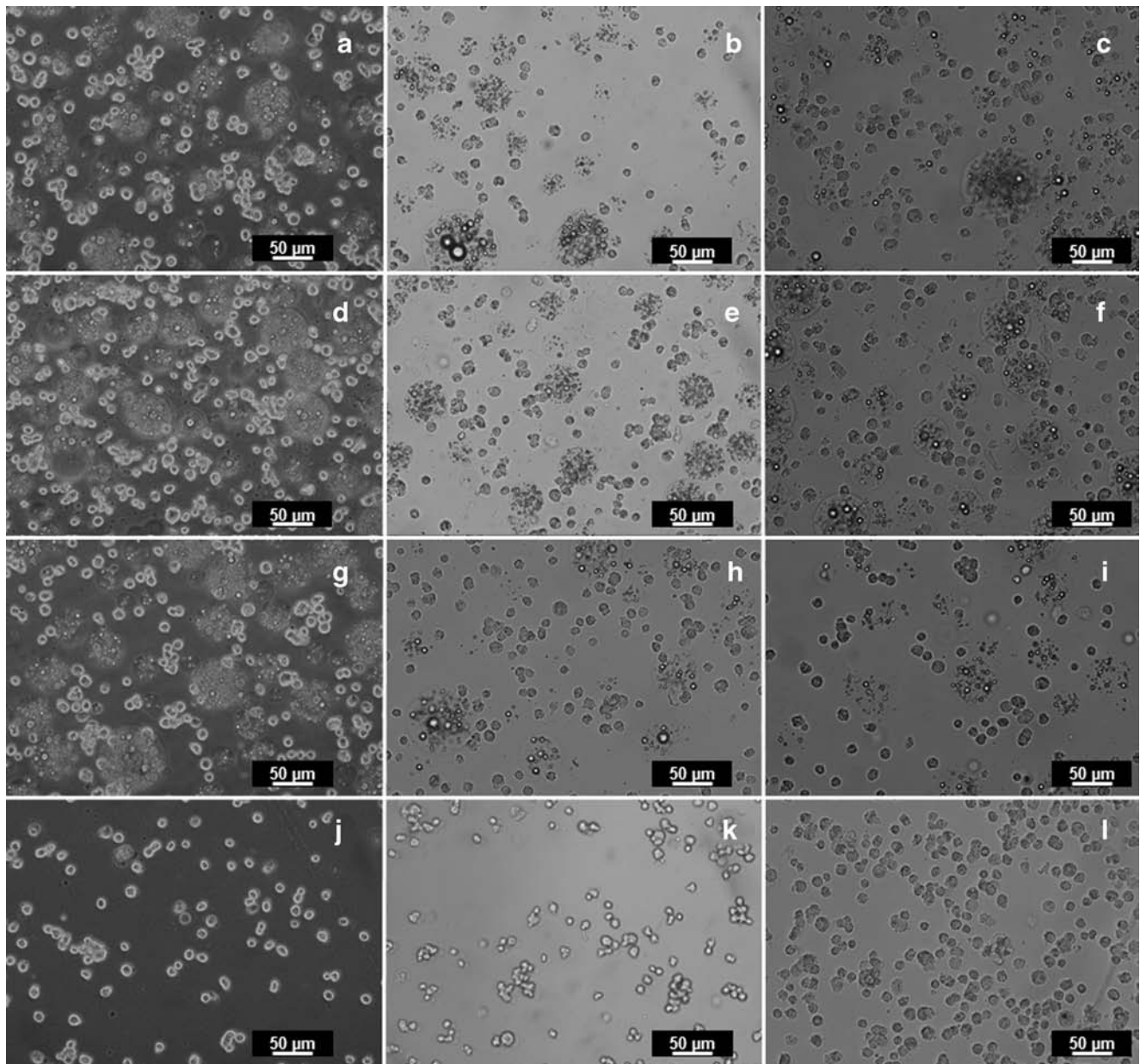


Fig. 8 Morphology of hMSCs for stability study in four media after different storage period at 4°C. Panel A, 0 h in medium A; panel B, 24 h in medium A; panel C, 48 h in medium A; panel D, 0 h in medium B; panel E, 24 h in medium B; panel F, 48 h in medium B, panel G, 0 h in medium C; panel H, 24 h in medium C; panel I, 48 h in medium C, panel J, 0 h in medium D; panel K, 24 h in medium D; panel L, 48 h in medium D.

Glucose release from microspheres was exponentially proportional to the released amounts from the dosage form offering fast release of glucose. Two main factors may affect the control of the glucose release, the porous structure and hydrophilic character of polymer. The hydrophilicity characteristics of the polymeric particles also contribute to the degradation rate, and hence, drug release.

According to cell viability results, although medium D showed better results at 48 h, our study demonstrate that it was the medium in which viability decreased more rapidly during the first hours, and thus the least suitable. These results

indicated greater cell viability in medium A in which glucose microspheres were included. Whilst, medium C was the least effective, buffer solution caused a rapid and significant decrease on cell viability. Statistically, medium A exhibited significant differences for the first 24 h when compared with other media. From 24 h up to 36 h, medium A presented better cell viability than C and D media ($P \leq 0.01$). After 36 h no significant differences were observed among A, B and D, being C the worst assayed medium.

In general, there was a progressive loss of viability but the results indicated that hMSCs had better survival rate when

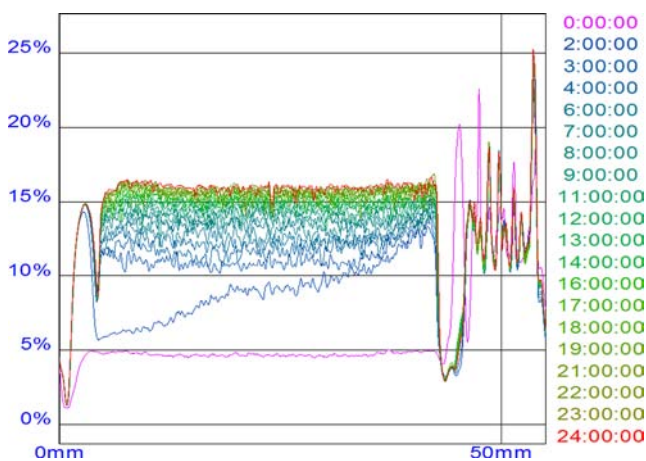


Fig. 9 Backscattering profile of the final cell product. The left side of the curve corresponds to the bottom of the vial, whereas the right side corresponds to the sample behaviour on the top.

they were packed in medium A until 30 h as compared to the packaging media B, C and D. Although the control medium is suitable as vehicle for MSCs, our study demonstrated greater cell viability in media with glucose microspheres for the first 30 h. Contrary, in medium C, with phosphate buffer, a greater decrease of cell viability during the first 36 h was observed when compared with A (without buffer). Thus, the results showed that the buffer solution caused a rapid and significant decrease of cell viability. As shown in Fig. 5b, the almost constant maintenance of cell viability was more evidenced in the parabolic than linear behavior; in this case, cell viability followed a downward trend from the first minutes. In contrary, the quadratic behaviors provided a constant cell viability, among them, medium A in a more stable and sustainable manner.

With regards to microbiological results, the inclusion of glucose loaded microspheres maintained the aseptic conditions of the final cell suspension. Similarly no immunophenotypic changes were observed in hMSC.

A rheological characterization was conducted in order to evaluate changes induced by the inclusion of glucose microspheres on the cell suspension. Rheological disturbances can play also an important role in the intramuscular administration of the final cell suspension. In fact, the viscosity of suspensions is closely related with physical and structural stability. Viscosity is also strongly influenced by factors such as aggregation of hMSCs. For this reason, the rheological characteristics of unstirred cell suspension were also studied. Cross was the mathematical equation that best fitted experimental data, it is a rheological model that combines four parameters and covers the entire shear rate range (39). As a rule, the four parameter models are difficult to apply because there is seldom enough data to allow good model fitting. However, they represent the best results in predicting the behavior of non-Newtonian fluids. These results may have important

implications for the administration because the success of the injection is dependent upon limiting shear forces of the needle wall causing cell lysis mainly produced by turbulent flow.

In relation to cell aggregation phenomena, images showed no overall cell aggregation (Fig. 8). However, in medium D after 24 h slightly cell aggregate signs could be seen. Therefore it can be concluded that the packaged finished medicinal product in medium A (containing glucose microspheres) did not exhibit hMSCs aggregation in suspension ensuring a good acceptance.

Stability evaluation is generally a crucial point in the scenario of advanced therapies. The long-term physical stability of cell-microspheres suspensions was tested by evaluating the photon backscattering profiles of the various samples. Turbiscan[®] Lab is considered as a device which predicts the stability, being able to detect destabilization before than the classical stability methods (microscopy, spectroscopy or turbidity). Moreover, it provides real-time information on the destabilization process based on the variation of backscattering. When sedimentation process is produced (migration of cells or microspheres from the top to the bottom), a backscattering increase *versus* time at the bottom of the sample is observed. When the sample suffers a creaming process, an increase of transmission *versus* time on the top of the vial is observed. If the destabilization phenomenon occurs due to aggregation (migration of cells from the bottom to the top), a backscattering increase *versus* time can be observed over the whole height of the sample (40). If backscattering profiles have a deviation of $\leq \pm 2\%$ it can be considered that there are no significant variations. Variations up to $\pm 10\%$ indicate instable formulations. The observed backscattering increase could be attributed to the sample flocculation (Fig. 9), possibly due to the formation of cells aggregates. The sedimented volume is high (the aggregates extend to roughly the whole volume of the suspension), it might be due to the particle size of the microspheres.

The open flocculi will settle slowly, and a long time will thus be needed for producing relatively compact sediments. Furthermore, because of the open structure of the aggregates, they will enclose comparatively large volumes of the supporting medium. Hence, the average particle-particle, cell-cell or particle-cell distances will be rather large, and the particles can get separated even after a mild shaking, so the suspensions will be easily re-dispersible. The peak that appeared at the top of the tube was indicative of creaming, presumably caused for migration of cellular components as lipid membranes from dead cells. Finally, after 11 h approximately there was no evolution in backscattering, indicating that the suspension was starting to stabilize.

It could be concluded that before the future administration, the injectable cell suspension should be re-dispersed just before using by gentle shaking in order to get a homogeneous hMSCs suspension, avoiding undesirable effects.

CONCLUSION

For the foreseeable future, cell therapy development will be based on not only in the search for new therapies but also in the study and design of these medicines. Particular attention will be paid to stability, safety and to expand the margins of use over time until administration.

The present study covers a comprehensive technological development of a packaging media. The media is composed of a nutrient (glucose) encapsulated into alginate microspheres. These particles are able to enhance the functionality of an hMSC suspension. For this reason, this strategy could be broadly applicable to various therapeutic approaches in which prolonged viability of cells is necessary. However, future works are claimed to improve the stability of cells during a longer period of time.

ACKNOWLEDGMENTS

Financial support from project MAT2011-26994 (MCNN-Ministerio de Ciencia e Innovacion) is acknowledged. This research work has been also partially funded by the CEI BioTIC Granada. We thank CABIMER's GMP Staff for cell preparation and characterization. Thanks are also extended to Dr Lyda Halbaut Bellowa from Barcelona University (Spain) for excellent technical expertise.

REFERENCES

1. Trounson A, Thakar RG, Lomax G, Gibbons D. Clinical trials for stem cell therapies. *BMC Med*. 2011;52:1–7.
2. Abdallah BM, Kassem M. Human mesenchymal stem cells: from basic biology to clinical applications. *Gene Ther*. 2008;15:109–16.
3. Phinney DG. Functional heterogeneity of mesenchymal stem cells: implications for cell therapy. *J Cell Biochem*. 2012;113:2806–12.
4. Le Blanc K, Mougiakakos D. Multipotent mesenchymal stromal cells and the innate immune system. *Nat Rev Immunol*. 2012;12:383–96.
5. Xiao N, Zhao X, Luo P, Guo J, Zhao Q, Lu G, *et al*. Co-transplantation of mesenchymal stromal cells and cord blood cells in treatment of diabetes. *Cytotherapy*. 2013;15:1374–84.
6. Da Silva JS, Hare JM. Cell-based therapies for myocardial repair: emerging role for bone marrow-derived mesenchymal stem cells (MSCs) in the treatment of the chronically injured heart. *Methods Mol Biol*. 2013;1037:145–63.
7. Miller RH, Bai L, Lennon DP, Caplan AI. The potential of mesenchymal stem cells for neural repair. *Discov Med*. 2010;9:236–42.
8. Wong KL, Lee KB, Tai BC, Law P, Lee EH, Hui JH. Injectable cultured bone marrow-derived mesenchymal stem cells in varus knees with cartilage defects undergoing high tibial osteotomy: a prospective, randomized controlled clinical trial with 2 year's follow-up. *Arthroscopy*. 2013;29:2020–8.
9. Titmarsh DM, Chen H, Glass NR, Cooper-White JJ. Concise review: microfluidic technology platforms: poised to accelerate development and translation of stem cell-derived therapies. *Stem Cells Transl Med*. 2013;2:946–2.
10. Chen Y, Yu B, Xue G, Zhao J, Li RK, Liu Z, *et al*. Effects of storage solutions on the viability of human umbilical cord mesenchymal stem cells for transplantation. *Cell Transplant*. 2013;22:1075–86.
11. Gálvez P, Clares B, Hmadcha A, Ruiz A, Soria B. Development of a cell-based medicinal product: regulatory structures in the European Union. *Br Med Bull*. 2013;105:85–105.
12. Brinckmann JE. Expanding autologous multipotent mesenchymal bone marrow stromal cells. *J Neurol Sci*. 2008;265:127–30.
13. Chen B, Wright B, Sahoo R, Connon CJ. A novel alternative to cryopreservation for the short-term storage of stem cells for use in cell therapy using alginate encapsulation. *Tissue Eng Part C Methods*. 2013;19:568–76.
14. Kelm JM, Fussenegger M. Scaffold-free cell delivery for use in regenerative medicine. *Adv Drug Deliv Rev*. 2010;62:753–64.
15. Bayoussif Z, Dixon JE, Stolnik S, Shakesheff KM. Aggregation promotes cell viability, proliferation, and differentiation in an in vitro model of injection cell therapy. *J Tissue Eng Regen Med*. 2012;6:e61–3.
16. Wang Y, Wei YT, Zu ZH, Ju RK, Guo MY, Wang XM, *et al*. Combination of hyaluronic acid hydrogel scaffold and PLGA microspheres for supporting survival of neural stem cells. *Pharm Res*. 2011;28(6):1406–14.
17. Bible E, Chau DY, Alexander MR, Price J, Shakesheff KM, Modo M. Attachment of stem cells to scaffold particles for intra-cerebral transplantation. *Nat Protoc*. 2009;4:1440–53.
18. Chen CH, Chang Y, Wang CC, Huang CH, Huang CC, Yeh YC, *et al*. Construction and characterization of fragmented mesenchymal-stem-cell sheets for intramuscular injection. *Biomaterials*. 2007;28:4643–51.
19. Gálvez-Martín P, Hmadcha A, Soria B, Calpena-Campmany AC, Clares-Naveros B. Study of the stability of packaging and storage conditions of human mesenchymal stem cell for intra-arterial clinical application in patient with critical limb ischemia. *Eur J Pharm Biopharm*. 2013. doi:10.1016/j.ejpb.2013.11.002.
20. Lane TA, Garls D, Mackintosh E, Kohli S, Cramer SC. Liquid storage of marrow stromal cells. *Transfusion*. 2009;49:1471–81.
21. Orive G, De Castro M, Kong HJ, Hernández RM, Ponce S, Mooney DJ, *et al*. Bioactive cell-hydrogel microcapsules for cell-based drug delivery. *J Control Release*. 2009;135:203–10.
22. Santos E, Pedraz JL, Hernández RM, Orive G. Therapeutic cell encapsulation: ten steps towards clinical translation. *J Control Release*. 2013;170:1–14.
23. Tran PH, Tran TT, Park JB, Lee BJ. Controlled release systems containing solid dispersions: strategies and mechanisms. *Pharm Res*. 2011;28(10):2353–78.
24. Parry RV, Chemnitz JM, Frauwirth KA, Lanfranco AR, Braunstein I, Kobayashi SV, *et al*. CTLA-4 and PD-1 receptors inhibit T-cell activation by distinct mechanisms. *Mol Cell Biol*. 2005;25:9543–53.
25. Dhanasekaran M, Indumathi S, Rajkumar JS, Sudarsanam D. Effect of high glucose on extensive culturing of mesenchymal stem cells derived from subcutaneous fat, omentum fat and bone marrow. *Cell Biochem Funct*. 2013;31:20–9.
26. Martín-Villena MJ, Fernández-Campos F, Calpena-Campmany AC, Bozal-de Febrer N, Ruiz-Martínez MA, Clares-Naveros B. Novel microparticulate systems for the vaginal delivery of nystatin: development and characterization. *Carbohydr Polym*. 2013;94:1–11.
27. De Vos P, De Haan BJ, Wolters GHJ, Strubbe JH, Van Schilfgaarde R. Improved biocompatibility but limited graft survival after purification of alginate for microencapsulation of pancreatic islets. *Diabetologia*. 1997;40:262–70.
28. Silva CM, Ribeiro AJ, Figueiredo IV, Gonçalves AR, Veiga F. Alginate microspheres prepared by internal gelation: development and effect on insulin stability. *Int J Pharm*. 2006;311:1–10.
29. Yamaoka K, Nakagawa T, Uno T. Application of Akaike's information criterion (AIC) in the evaluation of linear pharmacokinetic equations. *J Pharmacokin Biopharm*. 1978;6:165–75.

30. Louis KS, Siegel AC. Cell viability analysis using trypan blue: manual and automated methods. *Methods Mol Biol.* 2011;740:7–12.
31. European Pharmacopoeia sixth ed. Sterility 01/2008:20601. Strasbourg, France: Council of Europe; 2008. p. 155–158.
32. Petibotis C, Rigalleau V, Melin AM, Perromat A, Cazorla G, Gin H, *et al.* Determination of glucose in dried serum samples by Fourier-transform Infrared spectroscopy. *Clin Chem.* 1999;45:1530–35.
33. Otterlei M, Ostgaard K, Skjakbraek G, Smidsrod O, Soonshiong P, Espevik T. Induction of cytokine production from human monocytes stimulated with alginate. *J Immunother.* 1991;10:286–91.
34. Orive G, Ponce S, Hernandez RM, Gascon AR, Igartua M, Pedraz JL. Biocompatibility of microcapsules for cell immobilization elaborated with different type of alginates. *Biomaterials.* 2002;23:3825–31.
35. Silva CM, Ribeiro AJ, Figueiredo M, Ferreira D, Veiga F. Microencapsulation of Hb in chitosan-coated alginate microspheres prepared by emulsification/internal gelation. *AAPS J.* 2005;7:E903–13.
36. Chan ES, Wong SL, Lee PP, Lee JS, Ti TB, Zhang Z, *et al.* Effects of starch filler on the physical properties of lyophilized calcium–alginate beads and the viability of encapsulated cells. *Carbohydr Polym.* 2011;83:225–32.
37. Yuen CWM, Yip J, Liu L, Cheuk K, Kan CW, Cheung HC, *et al.* Chitosan microcapsules loaded with either miconazole nitrate or clotrimazole, prepared via emulsion technique. *Carbohydr Polym.* 2012;89:795–801.
38. Lecomte F, Siepmann J, Walther M, MacRae RJ, Bodmeier R. pH sensitive polymer blends used as coating materials to control drug release from spherical beads: elucidation of the underlying mass transport mechanisms. *Pharm Res.* 2005;22:1129–41.
39. Cross MM. Rheology of non-Newtonian fluids – a new flow equation for pseudoplastic systems. *J Colloid Sci.* 1965;20:417–37.
40. Fernández-Campos F, Calpena-Campmany AC, Rodríguez-Delgado G, López-Serrano O, Clares-Naveros B. Development and characterization of a novel nystatinloaded nanoemulsion for the buccal treatment of candidosis: ultrastructural effects and release studies. *J Pharm Sci.* 2012;101:3739–52.